EXPERIMENTAL YELLOW FEVER VIRUS INFECTION IN THE GOLDEN HAMSTER (*MESOCRICETUS AURATUS*) III. CLINICAL LABORATORY VALUES

ELENA SBRANA, SHU-YUAN XIAO, VSEVOLOD L. POPOV, PATRICK C. NEWMAN, AND ROBERT B. TESH*
Department of Pathology and Center for Biodefense and Emerging Infectious Diseases, University of Texas Medical Branch, Galveston, Texas

Abstract. Using a recently described hamster model of yellow fever (YF), we compared the hematologic and clinical chemistry changes that occur in blood with the histopathologic alternations observed in liver and other organs. Inflammatory foci and necroapoptotic hepatocytes were first observed in the liver three days after YF infection. This was accompanied by a rapid increase in serum transaminase and bilirubin values, elevation of prothrombin times, thrombocytopenia, and leukocytosis. Maximum liver pathology was observed on the sixth and seventh days post-infection; this corresponded to the peak alternations in clinical chemistry and hematologic values. In surviving hamsters, regenerating hepatocytes began to appear on the eighth day post-infection; this was accompanied by a corresponding return to baseline levels of most of the aforementioned clinical laboratory values. The histopathologic and clinical laboratory findings in the hamster model were very similar to those observed in severe human cases of YF. These results provide further validation of the utility of the hamster model for studying the pathogenesis and treatment of YF.

INTRODUCTION

Seventy years after the development of an effective and safe vaccine, yellow fever (YF) remains a significant public health threat in many areas of tropical Africa and America.[1] According to the World Health Organization, an estimated 200,000 cases of YF occur every year worldwide.[2] Most of the YF burden could be relieved by more effective vaccination practices because many of the countries where the disease is endemic only use vaccination as a reactive measure in emergency situations. Also, many travelers to disease-endemic regions do not receive the vaccine. Despite recent reports of YF vaccine–associated disease,[3] vaccination is the only practical and effective method to prevent YF among persons exposed to the virus. There is currently no specific treatment for the infection, and symptomatic cases generally receive only supportive care once they are admitted into a health care facility. Since most YF patients arrive at the hospital with advanced disease, it is seldom possible to obtain clinical data on the early stages of infection.

We have reported a hamster model of YF that has many similarities to severe YF in humans and macaques.[4,5] Hamsters are relatively inexpensive, and their care and maintenance are much simpler than rhesus monkeys, the animal species traditionally used for clinical studies of YF. We have used the hamster model to study the clinical, virologic, and pathologic aspects of the disease and to test potential therapeutics.[4–9] This report describes further studies of YF virus infection in the hamster model that address hematologic, coagulation, and clinical chemistry changes that occur during the disease.

MATERIALS AND METHODS

Virus. The hamster-virulent Jimenez strain of YF virus was used to infect the animals. This strain was previously described[4] and has had 11 serial passages in hamsters. Each animal received approximately 10^6 50% tissue culture infectious dose units of virus intraperitoneally. Three uninfected hamsters of the same age and sex served as controls.

Animals. The hamsters used in this study were 5–6-week-old female Syrian golden hamsters *(Mesocricetus auratus)* obtained from Harlan Sprague-Dawley (Indianapolis, IN). Animals were cared for in accordance with the guidelines of the Committee on Care and Use of Laboratory Animals (Institute of Laboratory Animal Resources, National Research Council) under an animal use protocol approved by the University of Texas Medical Branch. All work with infected animals and sera was carried out in biosafety level 3 facilities.

Sample collection. Beginning 24 hours after inoculation of YF virus, three hamsters were humanely killed each day for nine consecutive days to obtain blood and tissue samples for examination. The animals were first exsanguinated by cardiac puncture under deep halothane anesthesia (Hydrocarbon Laboratories, River Edge, NJ). The whole blood was saved for subsequent use in hematologic, coagulation, and clinical chemistry studies, as described below. A necropsy was then performed on the animals and samples of the following tissues were collected: liver, spleen, pancreas, kidney, adrenal gland, lung, heart, and intestine. Chunks of all tissues were fixed in 10% neutral-buffered formalin for 36 hours and then were transferred to 70% ethanol before being processed for routine paraffin embedding. Several 4–5-μm sections were made and stained with hematoxylin and eosin. Other unstained sections were use for immunohistochemical analysis and antigen detection, as previously described.[4]

A portion of fresh liver was also processed for ultrastructural studies as follows. Liver tissue was cut in a drop of fixative into pieces approximately 1 mm³ and fixed in a mixture of 2.5% formaldehyde, 0.1% glutaraldehyde, 0.03% trinitrophenol, 0.03% $CaC1_2$ in 0.05 M cacodylate buffer. Postfixation was done in 1% OsO4 in 0.1 M cacodylate buffer and *en bloc* staining was done in 1% uranyl acetate in 0.1 M maleate buffer. Sections were then dehydrated in ethanol and embedded in Poly/Bed 812 (Polysciences, Warrington, PA). Ultrathin sections were cut on a Reichert-Leica (Vienna, Austria) ultracut S ultramicrotome and examined with a Philips 201 electron microscope (Philips Electron Optics, Eindhoven, The Netherlands) at 60 kV.

Hematologic, biochemical, and coagulation studies. For coagulation studies, citrated blood was centrifuged at 2,500 × *g*
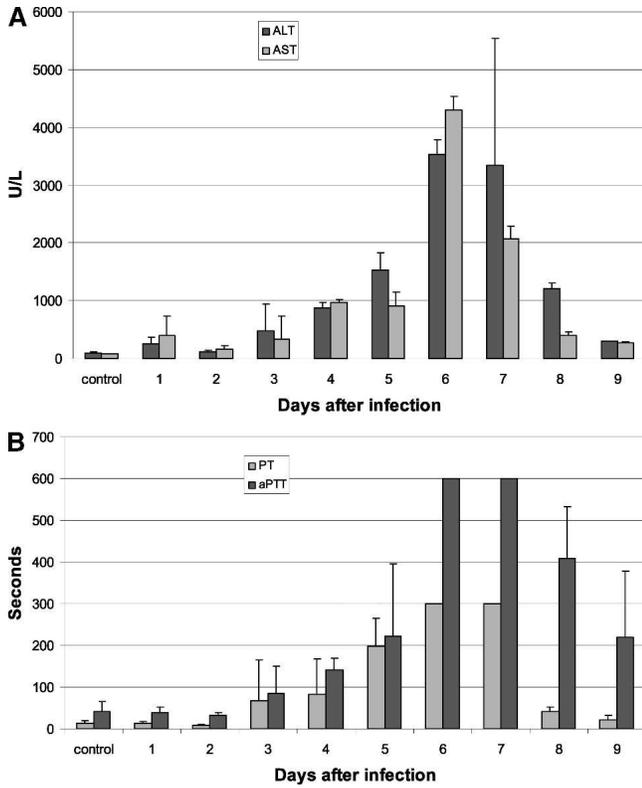
FIGURE 1. **A**, Daily mean + SD of alanine aminotransferase (ALT) and aspartate aminotransferase (AST) levels in sera of hamsters following infection with yellow fever virus. n = three animals/day. **B**, Daily mean + SD prothrombin time (PT) and activated partial thromboplastin time (aPTT) in hamsters following infection with YF virus. n = three animals/day.

for 10 minutes at 4°C. After centrifugation, the plasma was transferred into clean tubes and analyzed on a Star-t 4 coagulation analyzer (Diagnostica Stago, Parsippany, NJ). The following values were determined: prothrombin time (PT), activated partial thromboplastin time (aPTT), fibrinogen (FBG), and thrombin time (TT). Hematologic assays were performed directly on EDTA-treated whole blood using a Hemavet 950 analyzer (Drew Scientific, Oxford, CT) that determined counts of white blood cells (WBC), neutrophils (NE), monocytes (MO), lymphocytes (LY), basophils (BA), eosinophils (EO), red blood cells (RBC), and platelets (PLT), and hemoglobin (Hb) levels, and hematocrit (Hct). For clinical chemistry, whole blood without additives was allowed

to clot at room temperature for several hours and centrifuged for 5 minutes at 2,500 × g. Serum was transferred to clean tubes and analyzed promptly on a Prochem-V clinical chemistry analyzer (Drew Scientific), according to the manufacturer's instructions. The following biochemical parameters were determined: serum alanine aminotransferase (ALT), aspartate aminotransferase (AST), total bilirubin (TB), serum amylase, blood urea nitrogen (BUN), and serum potassium (K).

RESULTS

Clinical observations. During the first 3 days after infection, the hamsters' appearance and activity seemed normal. At necropsy, their organs also appeared grossly normal. By days 4 and 5 post-infection, the animals had become anorexic and lethargic. At necropsy, the spleen and liver were pale and soft. From the sixth day onward, most of the animals appeared emaciated and dehydrated. Spontaneous nosebleeds and diarrhea were also noted in some animals. Apart from the animals that were sampled, 24 additional hamsters died between days 6 and 9 post-infection. At necropsy, internal hemorrhages were frequently observed. The gross appearance and texture of the liver at this time was pale and soft, and the spleen was soft and enlarged (1.5–3 times).

Blood chemistry. No changes were observed in the daily values of BUN during the course of YF virus infection. In contrast, levels of serum transaminases (ALT and AST) showed a profound increase, reaching a maximum on day 6 post-infection of more than 3,500 U/L for ALT and almost 4,300 U/L for AST (Figure 1A and Table 1). A similar increase was observed in the TB and K levels, which both increased steadily from their baseline values to reach peaks on day 5 post-infection of 8 mg/dL and 7.5 mmol/L, respectively (Table 1). Albumin levels remained close to the baseline of 3.4 g/dL until day 5 post-infection when they decreased to 1.5–1.8 g/dL on days 6–8 post-infection, and then returned close to normal values on day 9 post-infection (Table 1).

Serum amylase values decreased beginning on approximately day 3 and remained low (compared with baseline levels) until day 9 post-infection (Table 1). These decreasing amylase levels may indicate some pancreatic malfunction or insufficiency during the acute phase of YF virus infection. In our earlier study of the pathology of YF virus infection in hamsters,[5] moderate-to-severe parenchymal necrosis was observed in the pancreas of infected animals beginning on day 5 post-infection.

Coagulation studies. Both PT and aPTT began to increase

TABLE 1
Clinical chemistry values in hamsters infected with yellow fever virus*

Clinical chemistry		Day after infection									
Test	Units	Control	1	2	3	4	5	6	7	8	9
ALT	U/L	98.2	259.3	109	478.7	879	1,529	3,536.7	3,336	1,202.6	296
AST	U/L	74.6	405	153.6	328.7	974.7	907.5	4,290	2,074.7	400	278
T-bilirubin	mg/dL	0.6	2.5	2.5	3.1	6.1	8	7.3	4.3	2.8	0.95
Albumin	g/dL	3.4	3.6	2.6	3.1	2.8	2.8	1.5	1.8	1.5	2.1
Potassium	mmol/L	3.8	4.2	3.9	4.6	4.9	7.5	5.7	3.8	3.4	4.2
BUN	mg/dL	27.7	23.7	19.3	19.3	18.7	17.7	54.3	26	13	19.5
Amylase	U/L	1,281.5	1,339.3	920.3	669	355.3	414	399.7	171	308	639

* ALT = alanine aminotransferase; AST = aspartate aminotransferase; T-bilirubin = total bilirubin; BUN = blood urea nitrogen. Values represent the mean obtained in three hamsters.
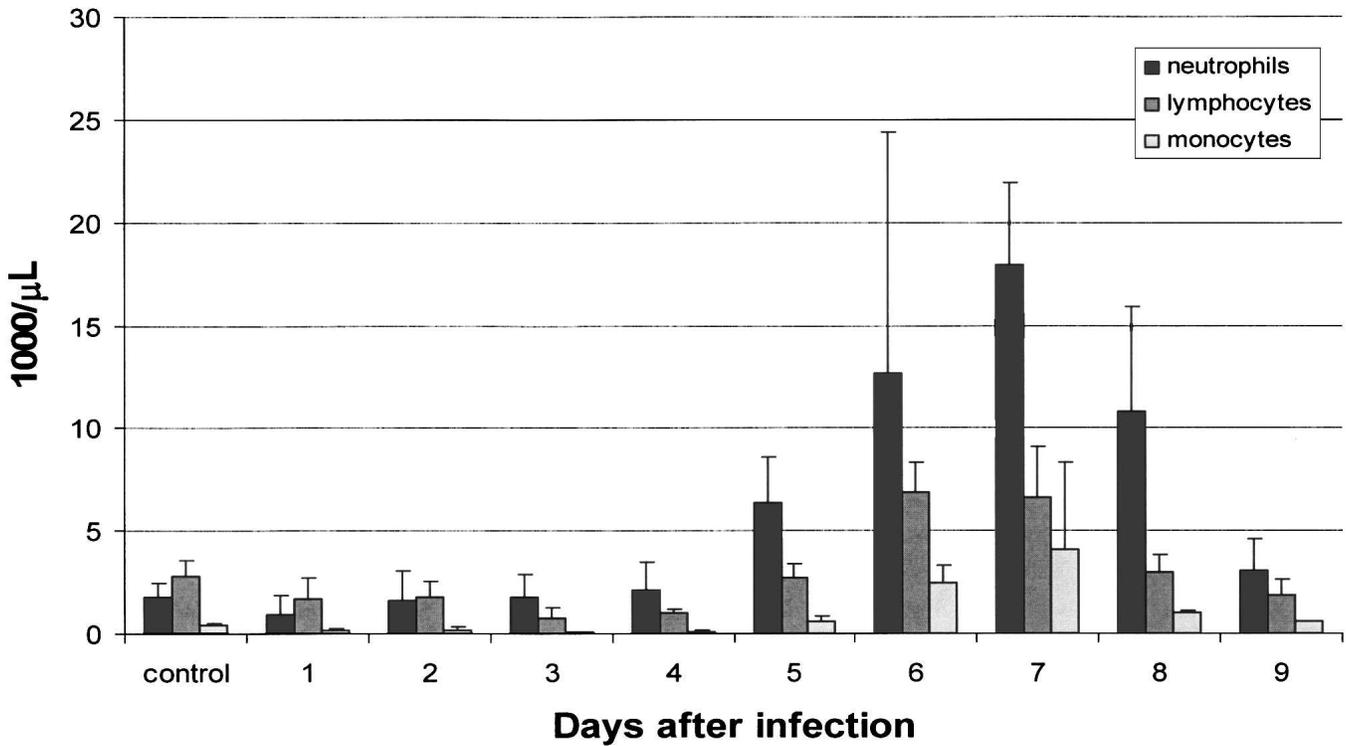
FIGURE 2.   Daily mean + SD counts of neutrophils, lymphocytes, and monocytes in the blood of hamsters following infection with yellow fever virus.

on day 3 post-infection, and by days 6 and 7 these values had increased to 600 and 300 seconds, respectively (Figure 1B). By day 9, the PT and aPTT values had decreased considerably, but they had not returned to normal levels. The FBG values were rather irregular and difficult to interpret. Baseline levels of 80 mg/dL were recorded on day 1. On days 2 and 3, the FBG increased to approximately 180 mg/dL. By day 7, the FBG values had decreased to less than 24 mg/dL, but they nearly returned to baseline (100 mg/dL) on day 9. TT values did not show a significant change during YF virus infection.

Hematologic studies. The principal hematologic changes in the infected hamsters were observed in the WBC and PLT. A slight leukopenia was observed on days 1–4 post-infection, but on day 5 post-infection the WBC began to increase, reach-

ing a maximum of 30,300/μL on day 7 post-infection. The WBC count then decreased to 5,600/μL on day 9 (Figure 2 and Table 2). Neutrophils represented the primary component of the WBC increase, but an increase also occurred in MO, LY, EO, and BA. The number of PLT remained at the baseline level of approximately 400,000/μL until day 4 post-infection. Thrombocytopenia occurred between days 4 and 7, but the PLT count had returned to nearly normal values by days 8 and 9 (Table 2). The RBC count, Hb level, and Hct did not change significantly during YF virus infection.

Histopathology. During the first two days after infection with YF virus, the hamster tissues appeared microscopically normal. On days 3 and 4 post-infection, spotty areas of hepatocytic apoptosis began to appear in the liver of infected ani-

TABLE 2
Hematologic findings in hamsters infected with yellow fever virus*

Hematology			Day after infection									
Test	Units	Control	1	2	3	4	5	6	7	8	9
WBC	K/μL	5.10	2.90	3.70	2.80	3.30	12.50	23.50	30.30	15.20	5.60
NE	K/μL	1.80	0.95	1.60	1.80	2.10	6.40	12.70	17.90	10.80	3.10
LY	K/μL	2.80	1.70	1.80	0.80	0.98	2.70	6.90	6.60	3.00	1.90
MO	K/μL	0.40	0.17	0.20	0.07	0.10	0.60	2.50	4.10	1.00	0.60
EO	K/μL	0.05	0.01	0.08	0.04	0.10	0.97	1.20	1.30	1.27	0.03
BA	K/μL	0.02	0.01	0.02	0.02	0.03	0.24	0.20	0.20	0.05	0.01
RBC	M/μL	5.10	4.40	4.90	5.70	6.00	6.50	4.80	5.50	5.80	7.10
Hb	g/dL	11.10	9.70	11.00	12.00	13.50	16.10	9.70	12.60	14.50	13.10
PLT	K/μL	410.50	396.70	363.30	474.00	191.70	276.00	176.00	168.70	331.00	399.50
MO/NE	(ratio)	0.22	0.18	0.13	0.04	0.05	0.09	0.20	0.23	0.09	0.19
MO/LY	(ratio)	0.14	0.10	0.11	0.09	0.10	0.22	0.36	0.62	0.33	0.32

* WBC = white blood cells; NE = neutrophils; LY = lymphocytes; MO = monocytes; EO = eosinophils; BA = basophils; RBC = red blood cells; Hb = hemoglobin; PLT = platelets. Values represent mean in three hamsters.
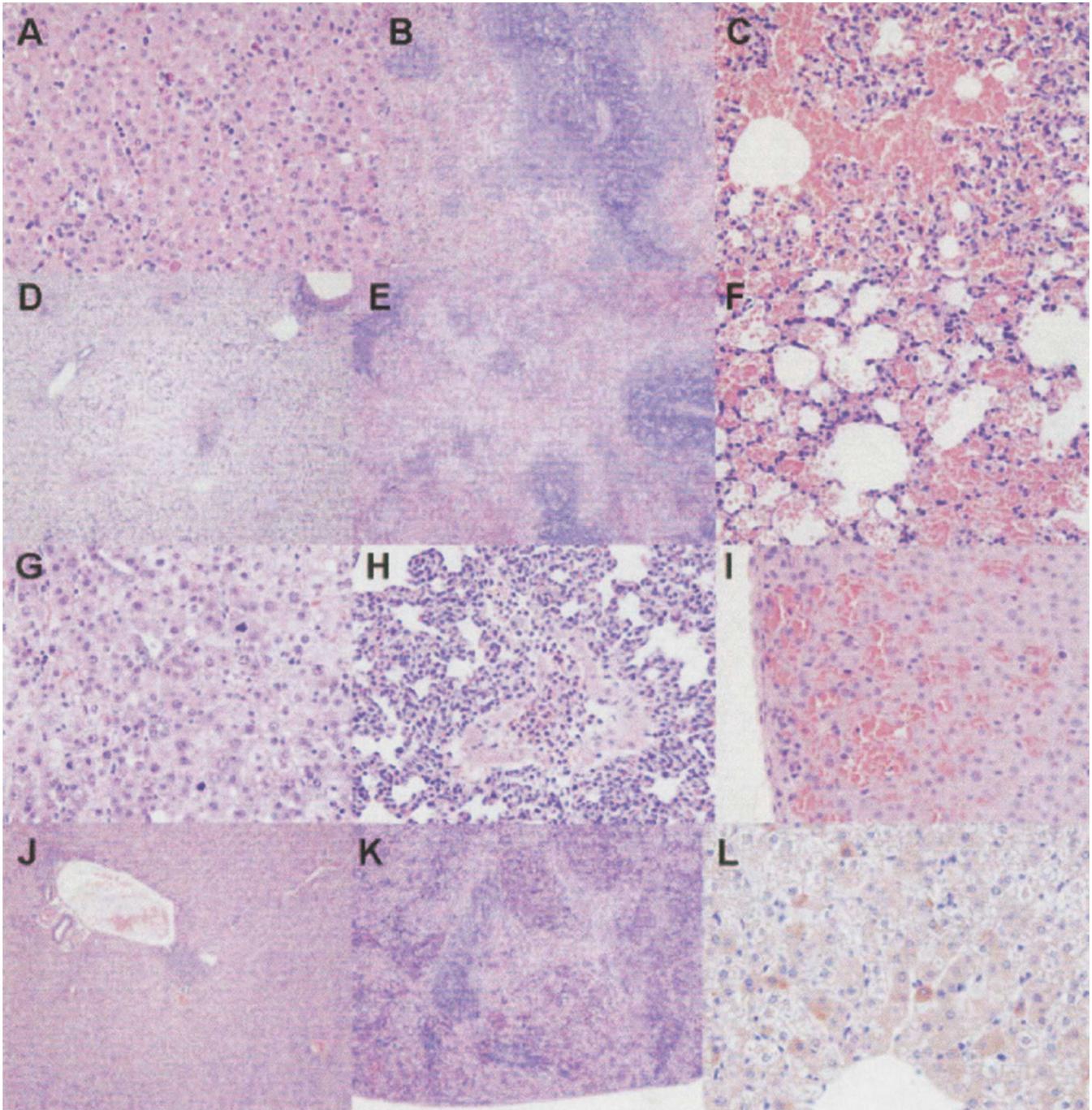
FIGURE 3. Photomicrographs of representative tissue sections from hamsters infected with yellow fever virus. **A**, Liver day 4 post-infection showing Councilman-like bodies. Some of the acidophilic bodies contain small dark pyknotic masses that probably represent residue from apoptosis of the original hepatocytes (original magnification × 400). **B**, Spleen day 3 post-infection showing lymphoid hyperplasia with disruption of the mantle and marginal zones; initial macrophage proliferation can be seen (original magnification × 100). **C**, Lung, day 4 post-infection showing pulmonary hemorrhage. (original magnification × 200). **D**, Liver day 6 post-infection showing periportal inflammation with mostly monocytes and lobular microvescicular steatosis (original magnification × 100). **E**, Spleen, day 5 post-infection showing marked lymphoid depletion with extensive proliferation of foamy macrophages containing cellular debris (original magnification × 100). **F**, Lung, day 6 post-infection showing pulmonary hemorrhage with several macrophages visible in the field (original magnification × 200). **G**, Liver day 8 post-infection showing mitotic figures and the ongoing regenerative process of the hepatocytes (original magnification × 400). **H**, Lung, day 7 post-infection showing immune cells, mainly monocytes, in a pulmonary vessel (original magnification × 200). **I**, Adrenal gland day 7 post-infection showing hyperemia and hemorrhage (original magnification × 400). **J**, Liver, day 9 post-infection showing regenerated hepatocyte plates and residual portal inflammation (original magnification × 100). **K**, Spleen, day 9 post-infection showing reconstitution of the normal splenic architecture with new follicles (original magnification × 100). **L**, Liver, day 4 post-infection showing infected hepatocytes containing yellow fever virus antigen (original magnification × 400). **A–K**, Hematoxylin and eosin stained; **L**, immunoperoxidase stained.

mals (Figure 3A). At the same time, lymphocytic hyperplasia was evident in the spleen, with an increase in splenic macrophages (Figure 3B). On day 4 post-infection, a few hemorrhagic infiltrates were observed in the lungs (Figure 3C). On days 5 and 6 post-infection, the liver showed mild inflammatory infiltrates in the portal tracts that contained mostly mononuclear leukocytes (Figure 3D). At this time, lobular microvesicular steatosis was observed in all animals, and many acidophilic bodies could also be seen. In the spleen (Figure 3E), lymphoid depletion became severe. Tangible body macrophages were diffuse in both the white pulp and red pulp and contained cellular debris. Lungs showed diffuse alveolar hemorrhage (Figure 3F). On days 7 and 8 post-infection, microvesicular fatty changes were still present in the lobular area of the liver, but hepatocytes had already begun to regenerate, as shown by the numerous mitotic figures found in all high-power fields (Figure 3G). The lungs of surviving animals did not show evidence of hemorrhage at this time; however, many mononuclear inflammatory cells were observed in the pulmonary blood vessels (Figure 3H). Scattered acidophilic bodies and hemorrhagic zones were also observed in the adrenal glands of two animals (Figure 3I).

By day 9 post-infection, lymphocytes were proliferating in the spleen, and the reconstituted white pulp gave the organ an almost normal appearance (Figure 3K). In the liver, most of the lobular areas showed regenerated hepatocytes, and scattered inflammatory foci were confined to the portal tracts.

No significant changes were observed in the heart or intestine of the animals included in the study. Mild-to-moderate changes were observed in the kidneys and adrenal glands, as previously described.[5]

Immunohistochemistry. From days 4 to 8 post-infection, viral antigen was observed in the liver of nearly all YF virus-infected hamsters (Figure 3L). The YF viral antigen–stained cells were also observed in the spleen of some infected animals on days 6 and 7 post-infection.

Transmission electron microscopy. Beginning on day 4 post-infection, microvesicular steatosis was observed in liver sections from the YF virus-infected hamsters, along with necroapoptosis of the infected hepatocytes (Figure 4).

DISCUSSION

In two previous publications,[4,5] we described the virology, immunology, and pathology of YF virus infection in hamsters. In this study, we investigated the hematologic, clinical chemistry, and coagulation changes that occur in hamsters during YF virus infection. The results obtained, as well as the histopathologic findings in the infected hamsters, were similar to those observed in severe human cases of the disease and in experimentally infected macaques.[1,10–17]

The first changes detected in the clinical chemistry values of the infected hamsters were an increase in the level of serum transaminases (Figure 1A). Both ALT and AST are markers of hepatocellular injury, although only ALT is unique to the liver. The abrupt increase in the both ALT and AST starting between days 3 and 4 was compatible with the histopathologic findings, namely that necroapoptotic hepatocytes were also observed on days 3 and 4 post-infection (Figure 3A). A similar pattern in the serum transaminase levels has been reported in severe human cases of YF; levels increase on the
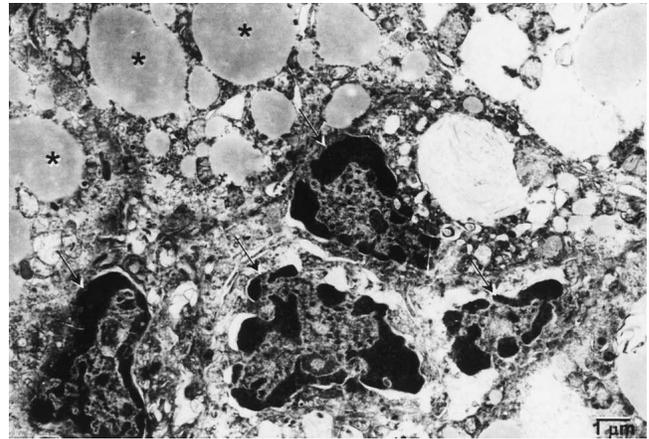

FIGURE 4. Transmission electron microscopy of ultrathin liver section from a hamster infected with yellow fever virus taken day 6 post-infection showing apoptotic hepatocytes (**arrows**) and accumulation of lipid droplets (**asterisks**) in the cytoplasm of viable hepatocytes.

second or third day of illness, peak 2–3 days later, and in surviving patients decrease rapidly over the next week or so.[1,14]

As shown in Figure 1B, an alternation of the PT and aPTT values occurred at approximately the same time as the increase in the serum transaminases. These changes are probably associated with the observed hepatocellular damage. The PT measures the integrity of the extrinsic and common pathways of coagulation (factors VII, X, and V; prothrombin; and fibrinogen). The aPTT measures the integrity of the intrinsic and common pathways of coagulation (high molecular weight kininogen; prekallikrein; factors VII, XI, IX, VII, X and V; prothrombin; and fibrinogen).[18] Since some clotting factors, such as factor VII, have half-lives of less than one day,[18] it is understandable why the PT and aPTT became abnormal shortly after the onset of hepatocellular damage and why they returned to baseline levels as hepatocellular regeneration began. Thrombocytopenia also occurred in the infected hamsters (Table 2) and followed a pattern similar to that observed with ALT, AST, PT and aPTT, although the relationship of thrombocytopenia to acute hepatocellular damage is unclear. Human cases of YF also have elevated prothrombin times and thrombocytopenia.[1] Both conditions undoubtedly contribute to the hemorrhagic phenomena associated with this disease.

The total WBC counts were increased in the infected hamsters between days 5 and 8 post-infection (Table 2 and Figure 2). Leukocytosis is indicative of an acute inflammatory process and consistent with the acute nature of YF virus infection. The WBC count reached a maximum on day 7 of more than $30,000/\mu L$. These laboratory values were supported by numerous inflammatory cells in blood vessels of the tissue sections.

All WBC components increased during YF virus infection, but the MO:LY and MO:NE ratios also increased (Table 2). This alternation in the ratio of cellular components of blood was also seen in spleen sections, where lymphocytes tended to disappear and splenic macrophages increased and engulfed the necrotic virus-infected cells and lymphocytes (Figure 3E). The mononuclear component also appeared to be predomi-

nant in the periportal inflammatory infiltrates seen in liver (Figure 3D), and many monocyte-macrophages were seen in sections of lungs on days 5–6 post-infection (Figure 3F). These findings are compatible with recent reports by Quaresma and others[16,17] based on histopathologic and immunohistochemical examination of livers from Brazilian cases of fatal YF. The histopathologic pattern observed in their patients was characterized by steatosis, lytic necrosis, and hepatocyte apoptosis associated with a mononuclear inflammatory infiltrate.[17] The inflammatory component in the livers consisted mainly of CD4+ T lymphocytes and smaller numbers of CD8+ T lymphocytes, CD20+ B lymphocytes, NKT+ cells, and S100+ dendritic cells in the midzonal sites of inflammation.[16,17] Based on these findings, they proposed that lymphocytes play an important role in the genesis of hepatic lesions in severe YF by inducing hepatocyte apoptosis through the binding to Fas receptors and release of cytokines.[16,17] Our findings tend to support their hypothesis.

The one notable difference in the pathogenesis of YF virus infection between hamsters and primates appears to be in the kidneys and heart. In humans and monkeys, the renal pathology associated with YF virus infection is characterized by eosinophilic degeneration and fatty change of the renal tubular epithelium without inflammation.[1] Renal failure is not uncommon. Eosinophilic degeneration and swelling of the tubular epithelial cells were noted in some of the hamsters, but it appeared to be transient.[5] Likewise, cloudy swelling and fatty changes have been observed in the heart of fatal human cases of YF;[1] however, the infected hamsters showed no specific pathologic abnormalities in the heart.[5] Nonetheless, the similarity of the histopathologic, hematologic, and clinical chemistry findings in both humans and hamsters infected with YF virus indicate that the hamster is a realistic, convenient, and inexpensive model for studies of the pathogenesis and treatment of YF.

Authors' address: Elena Sbrana, Shu-Yuan Xiao, Vsevolod L. Popov, Patrick C. Newman, and Robert B. Tesh, Department of Pathology, University of Texas Medical Branch, Galveston, TX 77555-0609.

Reprint requests: Robert B. Tesh, Department of Pathology, University of Texas Medical Branch, 301 University Boulevard, Galveston, TX 77555-0609, Telephone: 409-747-2431, Fax: 409-747-2429, E-mail: rtesh@utmb.edu.

REFERENCES

1. Monath TP, 2004. Yellow fever vaccine. Plotkin SA, Orenstein WA, eds. *Vaccines*. Fourth edution. Philadelphia: W. B. Saunders, 1095–1176.

2. World Health Organization, 1998. Distinct Guidelines for Yellow Fever Surveillance. Publication No. (WHO/EPI/GEN) 98.09. Geneva: World Health Organization. Available from http://www.who.int/emc-documents/yellow_fever/whoepigen9809c.html

3. Barwick RS, Marfin AA, Cetron MS, 2004. Yellow fever vaccine-associated disease. Scheld WM, Murray BE, Hughes JH, eds. *Emerging Infections 6*. Washington, DC: American Society for Microbiology Press, 25–34.

4. Tesh RB, Guzman H, Travassos da Rosa APA, Vasconcelos PFC, Dias LB, Bunnell JE, Zhang H, Xiao SY, 2001. Experimental yellow fever virus infection in the golden hamster *(Mesocricetus auratus)*. I. Virologic, biochemical, and immunologic studies. *J Infect Dis 183:* 1431–1436.

5. Xiao SY, Zhang H, Guzman H, Tesh RB, 2001. Experimental yellow fever virus infection in the golden hamster *(Mesocricetus auratus)*. II. Pathology. *J Infect Dis 183:* 1437–1444.

6. Xiao SY, Guzman H, Travassos da Rosa APA, Zhu HB, Tesh RB, 2003. Alteration of clinical outcome and histopathology of yellow fever virus infection in a hamster model by previous infection with heterologous flaviviruses. *Am J Trop Med Hyg 68:* 695–703.

7. Sbrana E, Xiao SY, Guzman H, Ye M, Travassos da Rosa APA, Tesh RB, 2004. Efficacy of post-exposure treatment of yellow fever with ribavirin in a hamster model of the disease. *Am J Trop Med Hyg 71:* 306–312.

8. McArthur MA, Suderman MT, Mutebi JP, Xiao SY, Barrett ADT, 2003. Molecular characterization of a hamster-viscerotropic strain of yellow fever virus. *J Virol 77:* 1462–1468.

9. McArthur MA, Xiao SY, Barrett ADT, 2005. Phenotypic and molecular characterization of non-lethal, hamster-viscerotropic strain of yellow fever virus. *Virus Res 110:* 65–71.

10. Kerr JA, 1951. The clinical aspects and diagnosis of yellow fever. Strode GK, ed. *Yellow Fever*. New York: McGraw-Hill Book Company, 385–425.

11. Elton NW, Romero A, Trejos A, 1955. Clinical pathology of yellow fever. *Am J Clin Pathol 25:* 135–146.

12. Monath TP, Brinker KR, Chandler FW, Kemp GE, Crupp CB, 1981. Pathophysiologic correlations in a rhesus monkey model of yellow fever. *Am J Trop Med Hyg 30:* 431–443.

13. del Rio C, Meier FA, 1998. Yellow fever. Nelson AM, Horsburgh CR, eds. *Pathology of Emerging Infections 2*. Washington, DC: American Society for Microbiology Press, 13–39.

14. Oudart JL, Rey M, 1979. Proteinurie proteinemie et transaminasemies dans 23 cas de fievre jaune confirmee. *Bull Wordl Health Organ 42:* 95–102.

15. Quaresma JAS, Barros VLRS, Fernandes ER, Pagliari C, Takakura C, Vasconcelos PFC, Andrade HF Jr, Duarte MIS, 2005. Reconsideration of histopathology and ultrastructural aspects of the human liver in yellow fever. *Acta Trop 94:* 116–127.

16. Quaresma JA, Barros VL, Pagliari C, Fernandes ER, Guedes F, Takakura CF, Andrade HF Jr, Vasconcelos PF, Duarte MI, 2006. Revisiting the liver in human yellow fever: virus-induced apoptosis in hepatocytes associated with TGF-β, TNF-α and NK cells activity. *Virology 345:* 22–30.

17. Quaresma JA, Barros VL, Fernandes ER, Pagliari C, Guedes F, Vasconcelos PF, Andrade HF Jr, Duarte MI, 2005. Immunohistochemical examination of the role of Fas ligand and lymphocytes in the pathogenesis of human liver yellow fever. *Virus Res 116:* 91–97.

18. Schafer AI, 2004. Approach to the patient with bleeding and thrombosis. Goldman L, Ausiello D, eds. *Cecil Textbook of Medicine*. 22nd edition. Philadelphia: W. B. Saunders, 975–979.